ISBN: 978-1-5386-7599-1
IEEE Catalog Number: CFP18R55-ART

PROCEEDINGS

# 2018 1ST INTERNATIONAL CONFERENCE ON BIOINFORMATICS, BIOTECHNOLOGY, AND BIOLOGICAL ENGINEERING (BioMIC) - BIOINFORMATICS AND BIOLOGICAL ENGINEERING

YOGYAKARTA, INDONESIA / 19–20 OCTOBER 2018

// Bioinformatics and Biological Data Mining symposium

// Biomedical Sciences and Engineering symposium

UNIVERSITAS GADJAH MADA
BADAN PENERBIT DAN PUBLIKASI

UGM BioMIC 2018

IEEE

IEEE INDONESIA SECTION

UGM BioMIC 2018

Badan Penerbit dan Publikasi Universitas Gadjah Mada
UGM Main Office Building, 3rd Floor, Room B3-02
Bulaksumur, Yogyakarta, Indonesia

(+62) 274 6491963
biomic@ugm.ac.id
http://biomic.ugm.ac.id
@biomicugm
biomicugm
flic.kr/biomic

# TABLE OF CONTENTS

## Bioinformatics and Biological Data Mining

# Biomedical Sciences and Engineering

# ORGANIZING COMMITTEE

BioMIC 2018

## **Advisory Board Committee**:

Dr. Piergiorgio Gentile

drg. Ika Dewi Ana, Ph.D.

Widodo, Ph.D.

## **Organizing Committee**:

**General Chair**
Dr. Tri Rini Nuringtyas

**Secretary**
Lisna Hidayati, M.Biotech.

**Publication Chair**
Dr. Sunu Wibirama

**TPC Chair**
Dr. I Wayan Mustika

**Treasury Chair**
Dr. Mutiah Amini

**Publicity Chair**

Dr. Igi Ardiyanto

Afiahayati, Ph.D.

Alva Edy Tontowi, Ph.D.

dr. Gunadi, Ph.D.

drg. Heni Susilowati, Ph.D.

**Local Organizing Chair**

Siti Uswatun Hasanah, STP.

**Local Program**

Muhammad Rafieiy, S.Si.

Suharman, S.E.

Alif Yuni Alfiani, S.Kom.

Rangga Kala Mahaswa, S.Fil.

Sulis Setiowati, M.Eng.

Galih Putri Wulandari, S.Farm.

# TECHNICAL PROGRAM COMMITTEE

## BioMIC 2018

Afiahayati (Universitas Gadjah Mada, Indonesia)

Adhistya Permanasari (Universitas Gadjah Mada, Indonesia)

Agung Setiawan (School of Electrical Engineering and Informatics ITB, Indonesia)

Anggoro Budi (Universitas Gadjah Mada, Indonesia)

Anis Nismayanti (Institute of Technology Sepuluh Nopember, Indonesia)

Dedy Yulianto (Universitas Gadjah Mada, Indonesia)

Dhimas Dharmawan (Nanyang Technological University, Singapore)

Dian Nurputra (Universitas Gadjah Mada, Indonesia)

Dwi Nugrahaningsih (Universitas Gadjah Mada, Indonesia)

Febri Susanto (Universitas Gadjah Mada, Indonesia)

Flandiana Yogianti (Universitas Gadjah Mada, Indonesia)

Gunadi (Universitas Gadjah Mada, Indonesia)

Hanggoro Rinonce (Universitas Gadjah Mada, Indonesia)

Heni Susilowati (Universitas Gadjah Mada, Indonesia)

Hevi Wihadmadyatami (Universitas Gadjah Mada, Indohnesia)

I Wayan Mustika (Universitas Gadjah Mada, Indonesia)

Igi Ardiyanto (Universitas Gadjah Mada, Indonesia)

Indra Mahayana (Universitas Gadjah Mada, Indonesia)

Indriana Kartini (Universitas Gadjah Mada, Indonesia)

Irfan Martiansyah (Indonesian Research Institute for Biotechnology and Bioindustry, Indonesia)

Jajah Fachiroh (Universitas Gadjah Mada, Indonesia)

Junaedy Yunus (Universitas Gadjah Mada, Indonesia)

Karna Wijaya (Universitas Gadjah Mada, Indonesia)

Lisna Hidayati (Universitas Gadjah Mada, Indonesia)

Made Rahmawaty (Universitas Gadjah Mada & Politeknik Caltex Riau, Indonesia)

2018 1st International Conference on Bioinformatics, Biotechnology, and Biomedical Engineering (BioMIC), Yogyakarta, Indonesia

# Biocomposite of Hydroxyapatite/Gelatin/PVA for Bone Graft Application

1st Alva Edy Tontowi
*Department of Mechanical and Industrial Engineering*
*Universitas Gadjah Mada*
Yogyakarta 55281, Indonesia
alvaedytontowi@ugm.ac.id

2nd Adhi Anindyajati
*School of Aerospace, Mechanical and Mechatronic Engineering*
*The University of Sydney*
NSW 2006, Australia
aani2456@uni.sydney.edu.au

3rd Rina Tangkudung
*Graduate School of Biomedical Engineering*
*Universitas Gadjah Mada*
Yogyakarta 55281, Indonesia
rinatangkudung@gmail.com

4th Punto Dewo
Department of Ortho & Traumatic
*Universitas Gadjah Mada*
Yogyakarta 55281, Indonesia
ortho@indo.net.id

***Abstract*—A porous block composite of Hydroxyapatite/Gelatin/Polyvynil Alcohol has been successfuly fabricated as a bonegraft. The porous block of composite was examined to investigate its compressive strength, micro structure and callus formation. Materials for the composite were hydroxyapatite synthesized from calcite (coHA), commercial hydroxyapatite (HA-200), gelatin (G) and polyvynil alcohol (PVA). The porous block composite was prepared from a solution, by mixing the loading material and distilled water with ratio of 5, 15 and 25% w/v. The loading material was made by blending of HA (coHA or HA-200), G and PVA with weight composition ratio of 1/1/0.15. To develop a porous block, the solution of composite was casted in a mold and freezed overnight prior to freeze-drying for 6 hours at 0.02 Bar and -50°C. Tests were performed on compression strength, microstructure, pore size and *in vivo*. The *in vivo* test was carried out by observing a callus growth within cancellous bone of white rat for 14 and 21 days. The results showed that the graft composed by coHA and HA-200 had average pore size of <10 µm up to 300 µm with compressive strength of 3 to 5 MPa. These strengths were in the range of trabecular bone strength. From the *in vivo* test, composite of [HA200/G/PVA] showed better callus growth compared to [CoHA/G/PVA] and the control.**

***Keywords—bonegraft, composite, porous, strength, in vivo.***

## I. INTRODUCTION

Bone graft based on apatite crystals have received increasing attention in bone tissue engineering applications due to their ability to preserve the structural and biological functions of the damaged hard tissues in a biomimetic way. Pay attention has also been made to address the problem in forming pure bioceramic powder as a base material for bone graft into acertain geometry that mimic a life bone. Bioceramic such as hydroxyapatite (HA) is bioactive material which is able to provide osteogenesis environment for growing the bone. Naturally, human bone contains about 69% of HA, organic materials and others [1]. Beyond the biological function, HA is also very important material as bone reinforcement that could supports the weight of the body. In the condition where the human bone is defect due to accidence or other diseases, the bone could be reconstructed mostly by bonegraft which is taken from another life bone within the same body (autograft). However, although this method has been claimed to be the most biocompatible one, it may cause weakness of the existing hard organ. For these reasons, therefore, the use of synthetic bone material or bonegraft such as hydroxyapatite (HA) and other Ca/P based materials might be promising biomaterial in the future. Sinthetic bioceramics like HA can be synthesised from various natural resources such as gypsum [2-4], calcite [5], bovine bone [4-7], corals [8], seashell [9], egg shell [10-12] and cattlefish bone [13,14]. Hydroxyapatite synthesizes could be carried out by hydrothermal [15,16] and sol-gel [17,18]. In the form of powder, a synthetic HA is difficult to be formed at room temperature into a certain shape and geometry, as it is hard and brittle. Shaping pure HA powder into a 3D part needs a sintering process at high temperature that typically at 1250 °C and more [19,20]. At this temperature, HA might change its phase into β-TCP or α-TCP which is easier to degrade. In order to avoid the phase change, all processes that uses HA as a base material have to be carried out at room temperature. In this, HA powder should be composed with other materials which acts as a matrix. Several matrix materials have been introduced, particularly natural and synthetic polymers such as collagen type-I, gelatin, PCL, PLA, PLLA, PMMA and many others. Among those materials, gelatin is one of a favorable material since it can be prepared easily from acid-treated collagens. Gelatin is biocompatible which is similar to collagen but is much cheaper to produce [21]. In addition, natural souces of gelatin can be found in the skins, tendons, cartilage, bones and other connectives tissue of animals [21]. Gelatin has been known as a material with high biocompatibility, biodegradability and bioactivity [22]. In the application, gelatin has been widely used as a material for producing medical products such as a wound dressings [23], a drug delivery systems [24], and by mixing it with PLGA, it could be used as an artificial nerves scaffold [25].

In developing biocomposite with gelatin as a matrix, gelatin plays important role in improving flexibility of the composite. In the porous form, it provides a favorable environment for cell

978-1-5386-7599-1/18/$31.00 ©2018 IEEE

to attach, proliferate and differentiate. Thus, composing HA powder into gelatin could generate a new biomaterial that has flexibility, good place for cell live and bioactive characteristic. This composite of [HA/gelatin] potentially could be used for scaffold application [26,27]. The composite with the same application could also be developed in the form of film by adding bioactive glass [28]. However, its mechnical strength is still weak and ease to swell in contacting with biological environment. To improve it, several additive materials have been proposed and applied as cross-linkers and binders. The cross-linker has function molecully to improve the link between molecules resulting the materials become stronger and better swelling resistance. Several cross-linkers have been introduced such as glutaraldehyde (GA) [26,27], genipin (GP) [28], enzym:mTGase [29]. In the case of gelatin, cross-linking with either GP or GA can improve their flexibility property and swelling resistance. Composite with gelatin-based material could also be prepared by adding it with polyvynil alcohol (PVA) for making hydrogel to be PVA/gelatin [30], chitosan/gelatin membran from hydrogel [31]. PVA is accounted to be crystalline polymer. The crystallinity within PVA can give beneficial as it can act as a chain crosslink for improving mechanical properties of the composite. However, in case the needs of lower crystallinity of PVA, the crystallinity can be easily reduced by blending PVA with hydrophilics component such as cyclodextrin, chitosan or carbon nanotube [31]. Composite based HA material also can be developed by composing it with other materials such as bioactive glass, chitosan, collagen, glass ionomer cement, photopolymer and others. Looking at the potensial of the existing materials and spirit to obtain better biocomposite which match to the application, this study aims to develop a biocomposite material that composed of HA, Gelatin and PVA [32,33].

## II. Materials and Method

### A. Materials

Materials used in this experiment were local hydroxyapatite CoHA, which was synthesized from natural calcite supplied by Bioceramics Universitas Gadjah Mada (UGM) and the commercial HA200 made by Tai Hei Chem-Co; Gelatin (G) from Merck, polyvynil alcohol (PVA) with molecular weight of 13,000 – 23,000 obtained from Sigma Aldrich, and distilled water.

### B. Preparation of Porous Block Composite [CoHA/G/PVA] and [HA200/G/PVA] and Sample for In Vivo.

The porous block composite samples were prepared as follows. Firstly, powders of CoHA, gelatin, and PVA were weighed with the weight ratio of 1:1:0.15. Total weight of this mixed powder over the distilled water volume then would be known as a solid loading (w/v). Secondly, the distilled water was prepared for solid loading ratios of 5, 15, 25% w/v. Thirdly, PVA powder was dissolved in distilled water and stirred at 300 rpm and 90 °C. At the same time, gelatin powder (G) was also dissolved at 300 rpm and 40 °C. Both solutions of PVA and gelatin were then mixed and stirred at 300 rpm. While still stirring at 300 rpm, HA powder was added little by little for few minutes until homogeneously mixed. The solution of [CoHA/G/PVA] was then casted in various mold kit size and froze at -20 °C in a freezer overnight before putting it in a freeze-dryer to obtain a porous block. Freeze drying was carried out at 0.02 Bar and -50 $^{o}$C for 24 hours. For compression test sample, the solution was casted in a mold kit with diameter of 6.1 mm and 12.1 mm high. This molding size was designed 0.1 mm higher to allow final sample size of 6 mm diameter and 12 mm long after shrinkage. While for *in vivo* test, the sample was casted in another mold kit with size of 2.1 mm height and 2.1 mm diameter, allowing shrinkage after solidifying. For [HA200/G/PVA] specimens,the same preparation procedures were carried out by replacing CoHA by HA200.

Sample for in vivo test was in cylinder shape, sized 2 mm in height and 2 mm in diameter. Thirty samples were prepared for 30 femurs bone of white rats (Wistar). Prior to implantation to the femur bone, the samples were colored with mallory and sterillized using gama-ray with 20 kGy dozes of radiation.

### C. Test Methods.

Tests were taken place including compressive test, microstructure, porosity and in vivo. Compressive test of the samples were carried out using Zwick Universal Testing Machine (Zwick Roell AG, Germany). The samples were in cylindrical shape with diameter of 6 mm and height of 12 mm. Compressive force was then applied to both ends of sample until the sample was broken (fractured). The compressive strength was calculated by applying equation 1 where $\sigma_c$ is the compression stress (MPa), $F$ is the force (Newton), and $A = (\pi d^2/4)$ is the crossed section area of the sample ($mm^2$) and d is the diameter of sample (mm).

$$\sigma_c = \frac{F}{A} \quad (1)$$

For microstructure observation, the samples were prepared using the same sample of compression stress. The sample was cut into two parts by breaking it gently to get a natural cross section. The surface of the cross section of the sample was kept in its natural condition. As the sample was non-conductive material, therefore, the sample need to be coated with gold using sputter coater for at least one cycle coating. If one cycle coating was resulted in unclear image, the coating can be repeated twice or more to get thicker coating. The gold coated sample was then placed on the specimen holder of the Scanning Electron Microscope (SEM) and ready to be scanned. Observation of the microstructure was carried out on the Scanning Electron Microscope (INSPEX S50, FEI Company, USA) at acceleration voltage of 7 to 10 kV.

Porosity ($\phi$) of the samples prepared in section #2.2 was calculated using Eq. 2:

$$\phi = 1 - \left(\frac{\rho_B}{\rho_S} x100\%\right) \quad (2)$$

where $\rho_B$ is the bulk density of the sample (sample mass divided by volume, in which the data was obtained from the sample measurement), $\rho_s$ is the solid density of the sample that could be calculated using rule of mixture in Eq. 3:

$$\frac{1}{\rho_S} = \frac{W_{HA}}{\rho_{HA}} + \frac{W_G}{\rho_G} + \frac{W_{PVA}}{\rho_{PVA}} \quad (3)$$

$W_{HA}$ is the mass fraction of HA, $W_G$ is the mass fraction of gelatin, $w_{PVA}$ is the mass fraction of PVA, $\rho_{HA}$ is the density of

HA (3.16 g/cm$^3$), $\rho_{gel}$ is the density of gelatin (1.037 g/cm$^3$), and $\rho_{PVA}$ is the density of PVA (1.329 g/cm$^3$). All data of the compressive and the porosity test were analyzed statistically using MANOVA.

The in vivo test was carried out by implanting the sterilized sample into femur bone of 30 white rats (Wistar) and measuring the growth rate of callus at 14$^{th}$ and 21$^{st}$ days periods. Thirthy white rat as animal test were grouped into 6 treatment groups including a control group. To measure the callus growth, a scoring method was applied and statistically analized using Kruskal Wallis for finding the differences of the group treatment. If there were any differences, analysis would be continued using Mann-Whithey method.

## III. Results and Discussion

### A. Compression Test

Results of compressive test for [coHA/G/PVA] and [HA200/G/PVA] composites for varying solid loading (5, 15, and 25 %w/v) was shown in Fig.1. In general, the average compressive strength increased proportionally by the increase of solid loading. For the solid loading of 5, 15, and 25% w/v, the compressive strength increased by 0.07 to 5.11 MPa respectively. The increase of the compressive strength occurred due to the increase of the density of the sample or due to reduced porosity as shown in the SEM results. The maximum compressive strength was obtained from the sample with 25% of solid loading. Sample with higher solid loading was not prepared due to mixing problem. Well-distributed HA particles were difficult to obtain within the solution. The highest compressive strength was still in the range of compressive strength of cancellous bone of distal femur and proximal tibia.

Similar to the compressive strength as seen in Fig.1 but in opposite direction was porosity. Fig. 2 showed porosity of [CoHA/G/PVA] and [HA200/G/PVA] composites. The porosity decreased from 96% to 82% following the increase of solid loading. Higher solid loading resulted in the more saturated solution, which reduced the gap between solid particles, lessen the amount of the voids, and decreased the sample porosity. This porosity, however, was still in the range of cancelleous/trabecular bone porosity of 50% to 95%. In examining the effect of different solid loading and types of HA on compressive strength and porosity using MANOVA, Kolmogorov-Smirnov test indicated that the data was normal. However, Box's M and Levene Test exhibited that the data was not homogenous as indicated by variance homogenity. Therefore, stricter alpha value was needed for univariate F-Test as described in reference [58], and the data was analyzed using Two-Way Anova with the alpha value of 0.01. Solid loading significantly affect porosity and compressive strength ($p<0.01$). Type of HA affected significantly compressive strength ($p<0.01$), but its effect on porosity was negligible as $p>0.01$ ($p=0.068$). If we look at the effect of interaction between solid loading-type of HA on porosity and compressive strength, there was no significant effect as indicated by $p=0.154$ (porosity) and $p=0.014$ (compressive strength). These statistical results were confirmed by the measured compressive strength and porosity depicted in Fig. 1 and 2. Additionally, Partial Eta Squared exhibited that solid loading provides the biggest effect on porosity and compressive strength for both [CoHA/G/PVA] and [HA200/G/PVA] composites.

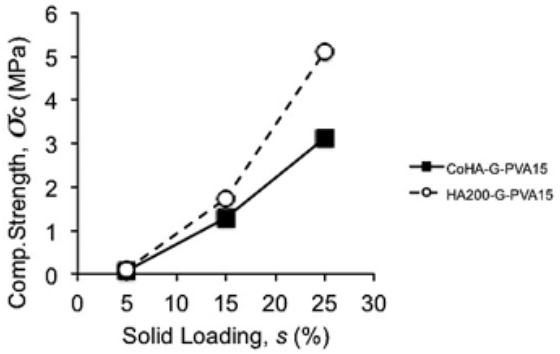


Fig. 1. Compressive Strength of [CoHA/G/PVA] and [HA200/G/PVA].

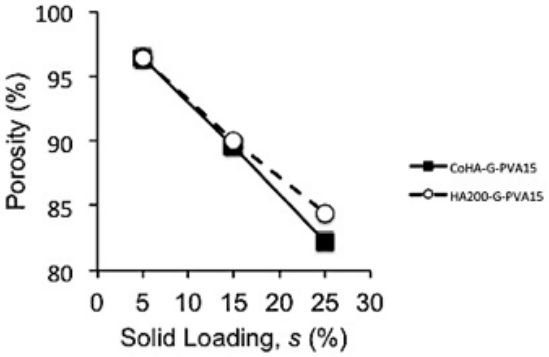


Fig.2. Porosity of [CoHA/G/PVA] and [HA200/G/PVA]

Considering the post hoc test on the effect of solid loading (5%, 15%, 25%) on porosity and compressive strength, all varying solid loading groups exhibited significant effect ($p<0.01$). The type of HA on composites (i.e. CoHA and HA200) contributed to the difference in compressive strength. Fig 1 showed noticeable differences at the solid loading of 25%. At this point, samples of [CoHA/G/PVA] and [HA200/G/PVA] exhibited physical differences as indicated by SEM results. Here, porosity of [CoHA/G/PVA] was higher than that of [HA200/G/PVA]. This difference might be caused by the uneven void formation or the air bubbles that trapped in the solution. Besides, HA200 had finer particle (5-20 μm) than CoHA (≤45 μm). Particle size may affect the mechanical strength of a composite. At a certain loading ratio, particles of hydroxyapatite with smaller size have larger surface area. This may increase the strength through more efficient stress transfer mechanism.

### B. Microstructure

The morphology, as shown in microscopic images of [coHA/Gel/PVA] and [HA200/G/PVA] composite for various solid loadings of 5, 15, and 25% w/v, were shown in Fig. 3 and 4, respectively. This morphology indicated clearly that the composites had pores with various sizes and shapes that potentially useful to acommmodate cell proliferation and biological function. The pores were formed by interconnected

wall composed of hydroxyapatite particles and matrix of [G/PVA].

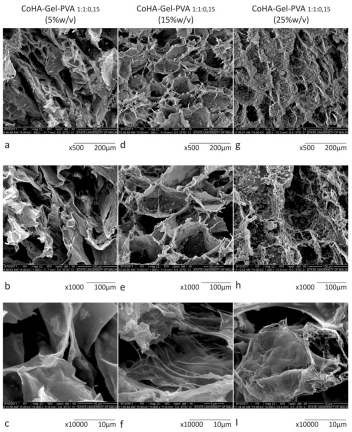


Fig.3. SEM of [CoHA/G/PVA] 5% (a-c), 15% (d-f), 25% (g-i)

In this composite, hydroxyapatite particles that distributed homogeneusly within a matrix of gelatin and PVA acted as reinforcement. The particles of hydroxyapatite were blanketed by [G/PVA] to form scaffold walls. Theoretically, PVA with its [–OH] group helps to engage hydroxyapatite and gelatine to get better bonding, which in return increases the strength [61]. SEM image of hydroxyapatite-gelatin-PVA at a larger magnification shows that the larger solid loading contributes to the thicker pore walls and rougher wall surface. Surface of [CoHA/G/PVA] tended to be more rugged than that of [HA200/G/PVA]. This might be caused by the smaller particle size of HA200 (5-10 µm) compared to CoHA (≤45 µm). Although the thickness of pore wall was not measured yet, the results of compressive strength, as shown in Fig. 2, have given evidence that solid loading had significant contribution in pore wall thickness, which also improved mechanical strength.

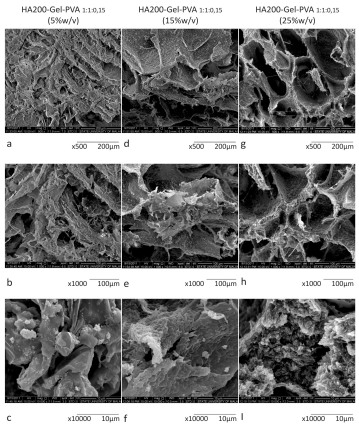


Fig.4. SEM of [HA200/G/PVA] 5% (a-c), 15% (d-f), 25% (g-i)

At each solid loading group, SEM images show that the macropore size is up to 300 µm and the micropore is <10 µm. In order to meet the requirement of scaffold for bone regeneration application, the porosity of the block composite should be around 80 to 90% with the pore size of 100-300 µm. Hence, based on Fig. 2 to 4, the porosity and pore size of the resulted scaffold are in the range of scaffold requirement. Therefore, the fabrication procedure used for forming the pores, has worked well. The pore walls, consisting hydroxyapatite (either coHA or HA-200) particles and gelatin/PVA matrix, appear as expected. Within the composite, particles of hydroxyapatite play a role as reinforcement, while the gelatin acts as a matrix and the PVA film as a linking reinforcement. In addition, particle shape of hydroxyapatite might be playing an important role in supporting different results on compressive strength and porosity. Achieving well-distributed particles within composite was more difficult with particles in thin and flat spike shapes (CoHA), compared to with particles in rounded stick figures (HA200). This occurred particularly for the solid loading of 25% w/v, although both sample types were prepared using the same method.

## *C. In Vivo*

The implantation of [CoHA/G/PVA] and [HA200/G/PVA] scaffold on the Wistar femur resulted in the transformation of bone tissue. Biological response which was affected by the scaffolds can be observed from the callus formation on bone tissue. Fig. 5 shows the callus formation on the treatment group and the control group. On the 14$^{th}$ day of observation, there was an increase in callus formation by 66.6%, 116.6 %, and 30% on the [CoHA/G/PVA] group compared to that of the control group, [HA200/G/PVA] to the control group, and [HA200/G/PVA] to the [CoHA/G/PVA] group, respectively. On the 21$^{th}$ day, the increase of callus formation was 71.4%, 85.7 %, and 50% on the [CoHA/G/PVA] group compared to the control group, [HA200/G/PVA] to the control group, and [HA200/G/PVA] to the [CoHA/G/PVA] group, respectively.

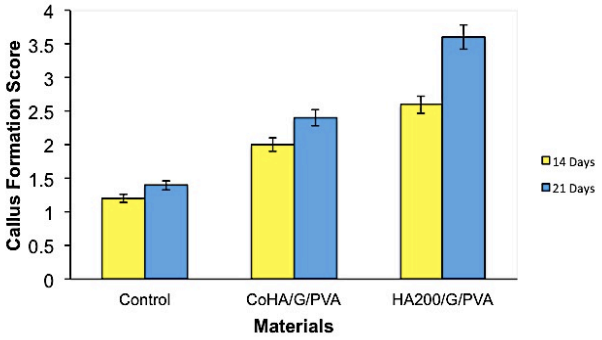


Fig. 5. Callus formation for various materials

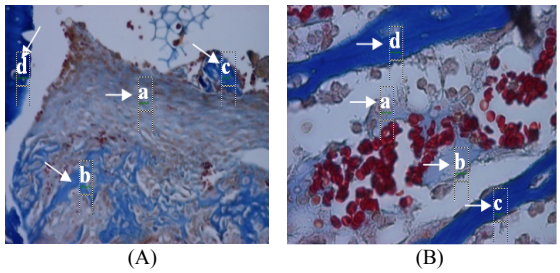


(A) (B)

***a:*** *connective tissue;* ***b:*** *hyaline cartilage;* ***c:*** *woven bone;* ***d:*** *trabecular bone*

Fig.6. Histological image of callus formation on the Wistar femur (control group) after 14 days (A) and 21 days (B), by Mallory coloring and 400x magnification.

Histological images of callus formation on the Wistar femur are shown in Fig. 6, 7, and 8. Fig. 6 indicates that the score of the control group on the 14th and 21st day was 1. Here, the callus image was dominated by many of connective tissues, few of hyaline cartilages, and woven bones. This excessive connective tissue caused a soft callus that might reduce the bone stiffness.

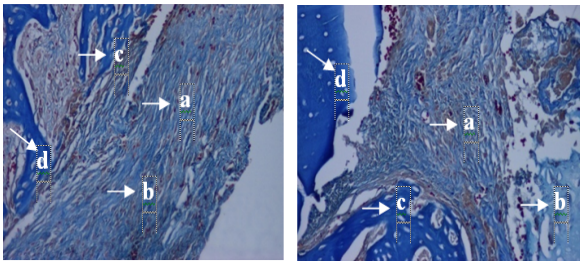


(A) (B)

***a:*** *connective tissue;* ***b:*** *hyaline cartilage;* ***c:*** *woven bone;* ***d:*** *trabecular bone*

Fig.7. Histological image of callus formation on the wistar femur [CoHA/G/PVA] group after 14 days (A) and 21 days (B), by Mallory coloring and 400x magnification.

Fig.7 shows the callus formation of the [CoHA/G/PVA] group on the 14th and 21st day. It represents histological images with score of 1-3, where hyaline cartilage are the more dominant composition, the trabecular and woven bone are better formed, and there is also fibrous connective tissue. The callus formations of the [HA200/G/PVA] group on the 14th and 21st day is shown in Fig. 8, in which the scores of the histological images were in between 2 to 4. This image indicates the dominance of woven bone and trabecular bone, with few of hyaline cartilage and connective tissue.

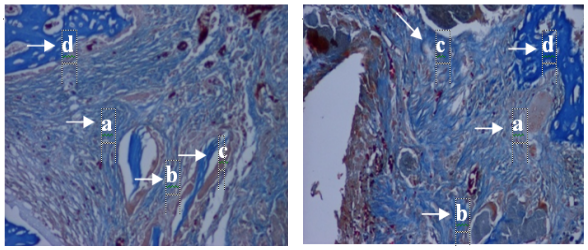


(A) (B)

***a:*** *connective tissue;* ***b:*** *hyaline cartilage;* ***c:*** *woven bone; d: trabecular bone*

Fig.8. Histological image of callus formation on the Wistar femur [HA200/G/PVA] group after 14 days (A) and 21 days (B), by Mallory coloring and 400x magnification.

Callus that has been fast re-mineralized will be reabsorbed and substituted by lamellar bone, so that the extremity function can be used sooner. This condition may cause the callus band to cross the crack line faster. On the stable bone crack with good blood supply, the perfect callus bone will be formed. The formed callus will further maturate with osteoblast activity, which the callus will transform into lamellar bone. The stable and rigid callus causing well blood supply on that area, which will inflict mesenchyme cells to differentiate into osteoblast, that will actively produces the woven bone. At the remodeling process, osteoblasts will fill the rooms between woven bones with trabecular bones, and will transform it into compact bone.

Statistically, the result of this study indicated that there was significant difference at the 14th and 21st day observation in which treatment groups had more callus than the control group. The average amount of callus formation showed that both at the 14th and 21st day, the [HA/G/PVA] group had the most calluses formed, whereas the control group had the least. This data explains that the porous block composite of [HA200/G/PVA] group at 21st day showed the better result. This composite had faster process of callus formation on the bone compared to that of [CoHA/G/PVA]. The particles of HA200 were evenly distributed and formed interconnected pores which were filled by fibrin matrix. Here, the osteogenic cells could migrate to the material surface easily. So, with this property, this material had similar composition with bone. Bone commonly is formed by 35% organic materials (protein in the form of collagen matrix) and 65% inorganic materials. The inorganic material mainly consists of calcium and phosphor that forms hydroxyapatite crystals.

## IV. Conclusions

In this study, a novel fabrication procedure of [HA/G/PVA] porous scaffold has been established with two different HA i.e. CoHA (local) and HA200 (commercial). Composite of [HA/G/PVA] has a comparable characteristic to trabecular bone and was capable of supporting callus formation. Varying solid loadings of 5, 15, 25% w/v affected compressive strength and porosity of the composite. The compressive strengths of 0.07 to 5.1 MPa achieved by the composite were in the range of trabecular bone strength. However, its porosities of 82-96 % was in the upper range of trabecular bone porosity. The porosities including micropores and macropores have size of <10 µm up to 300 µm. The *in-vivo* study also indicated that composite of [CoHA/G/PVA] was comparable to its counter part of [HA200/G/PVA) in improving callus formation. Finer particles with rounded shape like HA200 contributed a better result compared to CoHA which has coarser and spike particles shape. Furthermore, longer exposure time in examining callus formation is also needed in order to get better identification of apoptosis, understanding the role of inflammatory cells and bone cells. Over all, the composites made of those compositions were potential material to be used as a bone graft material.

## Acknowledgment

Part of this research was supported by research grant of Biomedical Engineering Graduate School and Department of Mechanical and Industrial Engineering UGM.

## References

[1] W. Suchaneck and M.Yoshimura, Processing and Properties of Hydroxyapatite Based Biomaterials for Use as Hard Tissue Replacemen Implant, Journal of Material Res. Vol.13, No.1 (1998) 94-117.

[2] S. Furuta, H. Katsuki and S. Komarneni, Porous Hydroxyapatite Monoliths from Gypsum Wast, Journal of Material Chem. No.8 (1998) 2803-2806.

[3] H. Katsuki, S. Furuta and S. Komarneni, Microwave versus Conventional Hydrothermal Synthesis of Hydroxyapatite Crystal from Gypsum, Journal of American Ceramics Society. Vol.87, No.8 (1988) 2257-2259.

[4] M.K. Herliansyah, E. Pujianto, M. Hamdi, A. Ide-Ektessabi, M.W. Wildan, and A.E. Tontowi, Preparation and Characterization of Natural Hydroxyapatite: Study of X-ray Diffraction Result from Bovine Bone Hydroxyapatite and Natural Gypsum Hydroxyapatite, Proceeding of International Conference on Product Design and Manufacture 2006, Department of Mechanical Engineering UGM Indonesia. (2006).

[5] M.K. Herliansyah, D.A. Nasution, M. Hamdi, A. Ide-Ektessabi, M.W. Wildan, and A.E. Tontowi, Preparation and Characterization of Natural Hydroxyapatite: A Comparative Study of Bovine Bone Hydroxyapatite and Hydroxyapatite from Calcite, Materials Science Forum Vol. 561-565 (2007) 1441-1444.

[6] N.A.M. Barakat, K.A. Khalil, F.A. Sheikh, A.M. Omran, B. Gaihre, M.S. Khil, H.Y. Kim, Physiochemical characterizations of hydroxyapatite extracted from bovine bones by three different methods: extraction of biologically desirable HAp, Mater Sci Eng. C 28 (2008a)1381–1387.

[7] N.A.M. Barakat, M.S. Khil, A.M. Omran, F.A. Sheik and H.Y. Kim, Extraction of pure natural hydroxyapatite from the bovine bones bio waste by three different methods, J Mater Proc Technol. 209 (2009) 3408–3415.

[8] M. Sivakumar, T.S.S. Kumart, K.L. Shantha, and K.P. Rao, Development of Hydroxyapatite Derived from Indian Coral, Biomaterials. 17 (1996) 1709-1714.

[9] K.S. Vecchio, X. Zhang, J.B. Massie, M. Wang, and C.W. Kim, Conversion of bulk seashells to biocompatible hydroxyapatite for bone implants, Acta Biomaterialia. 3 (1997) 910–918.

[10] E.M. Rivera, M. Araiza, W. Brostow, V.M. Castaño, J.R. Díaz-Estrada, R. Hernández, and J.R. Rodríguez, Synthesis of hydroxyapatite from eggshells, Materials Letters. 41 (1999) 128–134.

[11] S. Sasikumar, and R. Vijayaraghavan, Low Temperature Synthesis of Nanocrystalline Hydroxyapatite from Egg Shells by Combustion Method, Trends Biomaterial Artificial Organs. 19 (2006) 70-73.

[12] S.J. Lee and S.H. Oh, Fabrication of calcium phosphate bioceramics by using eggshell and phosphoric acid, Mater. Lett.. 57 (2003) 4570–4574.

[13] J.H.G. Rocha, A.F. Lemos, S. Kannan, S. Agathopoulos, and J.M.F. Ferreira, Hydroxyapatite Scaffolds Hydrothermally Grown from Aragonitic Cuttlefish Bones, Journal of Material Chemicals, 15 (2005) 5007–5011.

[14] H. Ivankovic, G.G. Ferrer, E. Tkalcec and M. Ivankovic, Preparation of Highly Porous Hydroxyapatite Ceramics from Cuttlefish Bone, Advances in Science and Technology, Trans Tech Publications, Switzerland. Vol.49 (2006) 142-147.

[15] X. Zhang, and K.S. Vecchio, Hydrothermal synthesis of hydroxyapatite rods, Journal of Crystal Growth. 308 (2007) 133–140.

[16] H. Katsuki, S. Furuta and S. Komarneni, Microwave versus Conventional Hydrothermal Synthesis of Hydroxyapatite Crystal from Gypsum, Journal of American Ceramics Society. Vol.87 No.8 (1998) 2257-2259.

[17] H.E. Hosseini, M.R. Housaindokht, and M. Chahkandi, Effects of parameters of sol–gel process on the phase evolution of sol–gel-derived hydroxyapatite, Materials Chemistry and Physics. 106 (2007) 310–316.

[18] I. Sopyan, Development of Hydroxyapatite Powders for Medical Applications via a Sol-Gel Procedure, Proceeding Asia-Pasific Nanotechnology Forum. (2004).

[19] A.E.Tontowi, Selective Laser Sintering and The Possibility of Processing Bioceramic Materials, Proc. The 4th International Seminar on Biomaterial, AUN/SEED-Net, 2-3 August 2004, Universiti Sains Malaya, Penang, Malaysia. (2004).

[20] S. Pramanik, A.K. Agarwal, K.N. Rai and A. Garg, Development of High Strength Hydroxyapatite by Solid-State-Sintering Process, Ceramics International. 33 (2007) 419–426.

[21] W. Yizao, W. Yulin and C. Guoxiang , Preparation and characterization of gelatin gel with a gradient structure, Polymer International. 49 (2000) 1600-1603.

[22] T. Nguyen and B. Lee, Fabrication and Characterization of Cross-linked Gelatin Electro Spun Nano-fiber, Journal of Biomedical Science and Engineering. 3 (2010) 1117-1124.

[23] Y.S. Choi, S.R. Hong and Y.M. Lee, Study on gelatin-containing artificial skin: I. Preparation and char-acteristics of novel gelatin-alginate sponge, Biomaterials, 20 (1999) 409-417.

[24] H. Akin and N. Hasircl, Preparation and Characterization of Crosslinked Gelatin Microspheres, Journal of Applied Polymer Science. 58 (1995) 95-100.

[25] L. Xiao-kun, C. Shao-Xi, L. Bin, Characteristics of PLGA-gelatin complex as potential artificial nerve scaffold, Colloids and Surfaces B: Biointerfaces. 57 (2007) 198-203.

[26] M.K. Narbat, F. Orang, M.S. Hashtjin and A. Goudarzi, Fabrication of Porous Hydroxyapatite-Gelatine Composite Scaffolds for Bone Tissue Engineering, Iranian Biomedical Journal. Vol.10 No. 4 (2006) 215-223.

[27] M. Azami, R. Mohammad and M. Fathollah, Gelatin/hydroxyapatite nanocomposite scaffolds for bone repair, Plastic Research On Line, Soscietty of Plastic Engineer. (2010).

[28] P. Gentile, V. Chiono, F. Boccafoschi, F. Baino, C. Vitale-Brovarone, E.Verne, N. Barbani and G. Ciardelli, Composite Films of Gelatine and Hydroxyapatite/Bioactive Glass tissue-Engineering Application, Journal of Biomaterials Science. 21 (2010) 1207–1226.

[29] G. Ciardelli, P. Gentile, V. Chiono, M. Mattioli-Belmonte, Enzymatically Crosslinked Porous Composite Matrices, Journal of Biomedical Materials Research Part A. (2009) 137-151.

[30] L. Yurong, M.G. Luke and J.F. Kennedy, Thermal behavior and mechanical properties of physically crosslinked PVA/Gelatin hydrogels, Journal of the Mechanical Behavior of Biomedical Materials. (2009).

[31] H. Nagahama, H. Maeda and T. Kashiki, Preparation and characterization of novel chitosan/gelatin membranes using chitosan hydrogel, Carbohydrate Polymers. 76 (2009) 255-260.

[32] A.E. Tontowi, M.K. Herliansyah, P. Dewo, P. Gentile and A. Anindyajati, Effect of PVA Coating on Diametral Tensile Strength of a Porous Block of Gelatine-Hydroxyapatite Composites, The 12th International Conference on QiR (Quality in Research). (2011).

[33] F. Wang, E. Guo, E. Song, P. Zhao, and J. Liu, Structure and properties of bone-like-nanohydroxyapatite/gelatin/polyvinyl alcohol composites, Advances in Bioscience and Biotechnology, 1 (2010) 185 18